*Anal. Chem.* **2001,** *73,* 2233−2238

# Surface-Induced Dissociation on a MALDI-Ion Mobility-Orthogonal Time-of-Flight Mass Spectrometer: Sequencing Peptides from an "In-Solution" Protein Digest

Earle Stone,[†] Kent J. Gillig,[†] Brandon Ruotolo,[†] Katrin Fuhrer,[‡] Marc Gonin,[‡] Albert Schultz,[‡] and David H. Russell*,[†]

*The Laboratory for Biological Mass Spectrometry, Department of Chemistry, Texas A&M University, College Station, Texas 77843, and Ionwerks Inc., 2472 Bolsover, Ste 255 Houston, Texas 77005*

**Peptide sequencing by surface-induced dissociation (SID) on a MALDI-ion mobility-orthogonal TOF mass spectrometer is demonstrated. SID of ∼100-fmol amounts of model peptides HLGLAR (*m*/*z* 666.8), gramicidin S (*m*/*z* 1142.5), and bovine insulin b chain (*m*/*z* 3495.5) was accomplished using hydrocarbon-coated gold grids and ∼20-eV collision energies. The current version of the instrument achieves a mobility resolution of ∼20 and TOF mass resolution better than 200. Peptide sequences of four peptides from a tryptic digest of cytochrome *c* (∼1 pmol deposited) were obtained. The advantage of IM-SID-o-TOF-MS is that a single experiment can be used to simultaneously measure the molecular weights of the tryptic peptide fragments (e.g., peptide mass mapping) and partial sequence analysis, (e.g., real-time tandem mass spectrometry.)**

Matrix-assisted laser desorption/ionization (MALDI) and time-of-flight mass spectrometry (TOF-MS) has evolved as an efficient tool for the analysis of thermally labile, nonvolatile biological compounds, especially peptides, proteins, RNA, and DNA.[1,2] MALDI-TOF-MS combined with peptide mass mapping is a powerful tool for the identification of proteins, and this technique is rapidly becoming the method of choice for proteomics;[3,4] however, the sample throughput requirements for proteomics places emphasis on rapid, efficient separation methods and accurate identification of the analyte. Recently we described a MALDI-ion mobility-orthogonal-(IM-o-)TOF-MS technique that provides rapid (100 $\mu$s−1 ms) gas-phase separations of tryptic digest fragments, and this method has excellent potential for peptide mass mapping.[5]

MALDI is a relatively "soft" ionization technique; thus, the abundance of structurally significant fragment ions is low and steps must be taken to induce fragmentation of the protonated peptide ions, $[M + H]^+$, to determine peptide sequences or sites of posttranslational modifications. Fragmentation of the ions can be increased by judicious choice of the MALDI matrix[6] or by using an ion activation process, e.g., collision-induced dissociation (CID),[7] photodissociation (PD),[8] or surface-induced dissociation (SID)[9] with subsequent mass analysis of the fragment ions, so-called MS−MS or tandem mass spectrometry. A drawback to traditional tandem mass spectrometry for application in proteomics is the requirement to mass select the analyte ions and then record individual fragment ion spectra.[10] The ideal tandem mass spectrometer would simultaneously acquire both the $MS^1$ and $MS^2$ spectra.[11]

One approach to the ideal tandem mass spectrometer is to couple ion mobility to TOF mass spectrometry.[12] Ion mobility gives rapid separation (100 $\mu$s−20 ms per elution cycle) of gas-phase ions, and separation is achieved on the basis of size, viz. volume-to-charge ($V/z$) (assuming that the interaction potential is negligible).[13] For example, Griffin et al. showed that the mobility of structurally related compounds decreases almost linearly with mass and the standard error in a mass-mobility correlation can be as low as ±2%.[14] Berant and Karpas[15] also showed that a mass-mobility correlation exists and that inclusion of an empirical, mass-

[†] Texas A&M University.

[‡] Ionwerks Inc.

(1) Kowalski, P.; Stoerker, J. *Pharmacogenomics* **2000**, *1* (3), 359−366.
(2) Shevchenko, A.; Loboda, A.; Shevchenko, A.; Ens, W.; Standing, K. G. *Anal. Chem.* **2000**, *72* (9), 2132−2141.
(3) Humphery-Smith, I.; Cordwell, S. J.; Blackstock, W. P. *Electrophoresis* **1997**, *18* (8), 1217−1242.
(4) Corthals, G. L.; Gygi, S. P.; Aebersold, R.; Patterson, S. D. In *Proteome Research: Two-Dimensional Gel Electrophoresis Detection Methods*; Rabilloud, T., Ed.; Springer-Verlag: Berlin, Germany, 2000; pp 197−231.
(5) Gillig, K. J.; Ruotolo, B. T.; Stone, E. G.; Russell, D. H.; Fuhrer, K.; Gonin, M.; Schultz, A. J. *Anal. Chem.* **2000**, *72* (17), 3965−3971.
(6) Kinsel, G. R.; Preston, L. M.; Russell, D. H. *Biol. Mass Spectrom.* **1993**, *23*, 205−211.
(7) Cooper, H. J.; Derrick, P. J. In *Mass Spectrometry in Biomolecular Sciences*; Capprioli, R. M., Malorni, A., Sindona, G., Eds.; NATO ASI Series, Series C 475; Kluwer Academic Publishers: London, 1996; pp 201−259.
(8) Barbacci, D. C.; Russell, D. H. *J. Am. Soc. Mass Spectrom.* **1999**, *10* (10), 1038−1040.
(9) Cooks, R. G.; Miller, S. A. In *Fundamentals and Applications of Gas-Phase Ion Chemistry*; Jennings, K. R., Ed.; NATO ASI Series, Series C 521; Kluwer Academic Publishers: London, 1999; pp 55−114.
(10) Figeys, D.; Corthals, G. L.; Gallis, B.; Goodlett, D. R.; Ducret, A.; Corson, M. A.; Aebersold, R. *Anal. Chem.* **1999**, *71* (13), 2279−2287.
(11) McLafferty, F. W. In *Tandem Mass Spectrometry*; McLafferty, F. W., Ed.; John Wiley and Sons: New York, 1983; pp 1−10.
(12) (a) Creaser, C. S.; Benyezzar, M.; Griffiths, J. R.; Stygall, J. W. *Anal. Chem.* **2000**, *72*, 2724−2729. (b) Eiceman, G. A.; Bergloff, J. F.; Rodriquez, J. E.; Munro, W.; Karpas, Z. *J. Am. Soc. Mass Spectrom.* **1999**, *10*, 1157−1165. (c) Hoaglund-Hyzer, C. S.; Li, J.; Clemmer, D. E. *Anal. Chem.* **2000**, *72*, 2737−2740.
(13) Tammet, H., *J. Aerosol Sci.* **1995**, *26* (3), 459−75

10.1021/ac001430a CCC: $20.00 
Published on Web 04/05/2001

dependent correction factor in Mason's collision cross-section equation gave quantitative agreement between mobilities and mass. Clemmer showed similar results for both doubly and singly charged peptide ions formed by electrospray ionization.[16] Here we show a near-linear relationship exists between total drift time and $m/z$ for the typical mass range of tryptic digest fragment ions, e.g., $m/z$ 500−3000.

SID can be combined with IM-o-TOF-MS by inserting a metal surface between the mobility drift cell and the ion source of the o-TOF. SID is the result of inelastic collisions between the ion and surface, and the fragmentation efficiency is very high. For example, SID efficiencies, defined in terms of fragment ion abundances, of greater than 10% have been reported.[9] For low-energy (10−200 eV) collisions with a surface, Cooks suggested that unimolecular dissociation of the activated ions occurs in the gas phase after leaving the surface.[17] Recent results by Hanley et al. for cyclic peptide ions are consistent with this view and show that the SID fragment ions leave the surface with a range of kinetic energies and a common velocity.[18] Energy deposition by SID is variable with experimental conditions, but the two most important parameters are the translational energies of the ion and the angle of incidence. Cooks and Wysocki have argued that ions activated by low-energy collisions with a surface have relatively narrow internal energy distributions, and the internal energy distributions have some dependence on the nature of the surface.[19,21] Laskin et al. showed that the internal energy distributions of ions activated by SID are very similar to ions activated by multiple-collisional activation CID.[22] Internal energies of ∼4 eV fwhm have been reported, and the most probable internal energies increase as the kinetic energies of the incident ion increases. Thus, SID provides "tunability" to the fragmentation chemistry and can be accomplished with much finer control than is possible with CID. Regardless of the details, SID spectra are more reproducible than CID spectra recorded under similar experimental conditions.[21,22]

In this work, we discuss the implementation of SID in MALDI-IM-o-TOF-MS for the purpose of acquiring sequence-informative fragment ion spectra simultaneous with the acquisition of the peptide mass map of complex peptide mixtures, e.g., mixtures of peptides generated by proteolytic digestion of proteins. The IM-o-TOF instrument is similar to the TOF-TOF instrument used by Cooks et al.[23] for SID studies. That is, the ions are activated in a field-free region between $MS^1$ and $MS^2$; thus, the fragment ions are formed by unimolecular dissociation prior to entering the ion source of the o-TOF. The advantage of this approach is that the fragment ions can be detected by linear and reflectron TOF as "in-source" fragment ions.[24] Additionally, the drift times for mobility (100 $\mu$s−20 ms) are significantly longer than for TOF mass analysis (5−50 $\mu$s); thus, the MS−MS experiment can be acquired in real time. TOF-MS data from the peptide mass map and SID fragment ion spectra can be used to identify the protein by searching a protein database. With as few as one tryptic digest fragment over $m/z$ 2000 and one SID fragment that does not represent the loss of lysine or arginine, species-specific protein identification can be obtained.[25] By automating sample handling, providing computer selection of informative peaks, and linking the end result to an Internet database search, very high identification rates can be achieved.[26]

## EXPERIMENTAL SECTION

The instrument used for these studies has been described previously.[5] The instrument was modified for SID by positioning a hydrocarbon-coated (adventitious pump oil) gold grid (Buckbee-Mears, St. Paul, MN) in-line (perpendicular to the ion beam) between the mobility drift cell and the extraction plates of the o-TOF source.[27,28] Several grids, 300 lines/ per in., 90% transmittance, were overlaid to reduce the transparency to ∼30%. This design was chosen based on convenience for performing SID and IM-TOF measurements on the same instrument. A new instrument with improved mobility resolution (20 to ∼100) and mass resolution (200 to ∼2000) is currently under construction. The ion mobility chamber was maintained at 5 Torr He with a field strength of 10 V $cm^{-1}$. SID was performed at a grazing incidence angle[29] to the surface and at collision energies ranging from 20 to 90 eV. The TOF mass spectrometer was calibrated using a mixture of six peptides: HLGLAR (MW 665.8), des-$Arg^9$-bradykinin (MW 904.0), neurotensin fragment 1−8 (MW 1030.1), gramicidin S (MW 1141.5), substance P (MW 1347.6), and RRLIEDAQKAARG (MW 1519.7). Studies were performed on single peptides, peptide mixtures, and protein digests.

The horse heart cytochrome *c* and peptides used in the study were purchased from Sigma Chemicals Co. (St. Louis, MO) and dissolved in methanol without further purification. Sequencing grade trypsin was purchased from Promega (Madison, WI) and used in a 40:1 (w/w) analyte-to-trypsin ratio. Cytochrome *c* was dissolved in aqueous 50mM ammonium bicarbonate (Sigma) to make a 1 $\mu$M peptide solution. The protein/enzyme solution was incubated at 37° C for 3 h, quenched in ice, and then stored in a freezer. The matrix was composed of equal parts of α-cyano-4-hydroxycinnamic acid (α-cyano) and fructose (Aldrich, Milwaukee,


(14) Griffin, G. W.; Dzidic, I.; Carroll, D. I.; Stillwell, R. N.; Horning, E. C. *Anal. Chem.* **1973**, *45* (7), 1204−1209.
(15) Berant, Z.; Karpas, Z. *J. Am. Chem. Soc.* **1989**, *111* (11), 3819−3824.
(16) Valentine, S. J.; Counterman, A. E.; Hoaglund, C. S.; Reilly, J. P.; Clemmer, D. E. *J. Am. Soc. Mass Spectrom.* **1998**, *9* (11), 1213−1216.
(17) Cooks, R. G.; Miller, S. A. In *Fundamentals and Applications of Gas-Phase Ion Chemistry*; Jennings, K. R., Ed.; NATO ASI Series, Series C 521; Kluwer Academic Publishers: London, 1999; pp 85−87.
(18) Schultz, D. G.; Lim, H.; Garbis, S.; Hanley, L. *J. Mass Spectrom.* **1999**, *34* (3), 217−225.
(19) Cooks, R. G.; Ast, T.; Mabud, M. A. *Int. J. Mass Spectrom. Ion Processes* **1990**, *100*, 209−265.
(20) Despeyroux, D.; Wright, A. D.; Jennings, K. R., *Int. J. Mass Spectrom. Ion Processes* **1993**, *126*, 95−99.
(21) (a) McCormack A. L.; Somogyi A.; Dongre A. R.; Wysocki V. H. *Anal. Chem.* **1993**, *65* (20), 2859−2872. (b) Kane, T. E.; Angelico, V. J.; Wysocki, V. H. *Langmuir* **1997**, *13* (25), 6722−6725.
(22) Laskin, J.; Denisov, E.; Futrell, J. *J. Phys. Chem. B* **2001**, *105* (9), 1895−1900
(23) Bier, M. E.; Amy, J. W.; Cooks, R. G.; Syka, J. E. P.; Ceja, P.; Stafford, G. *Int. J. Mass Spectrom. Ion Processes* **1987**, *77* (1), 31−47.
(24) *Time-of-Flight Mass Spectrometry: Instrumentation and Applications in Biological Research*; Cotter, R. J., Ed.; American Chemical Society: Washington, DC, 1997; pp 195−198.
(25) Pappin, D. J. C.; Hojrup, P.; Bleasby, A. J. *Curr. Biol.* **1993**, *3* (6), 327−332.
(26) Schrotz-King, P.; Wilm, M.; Andersen, J. S.; Ashman, K.; Podtelejnikov, A. V.; Bachi, A.; King, A.; Mann, M. *J. Recept. Signal Transduction Res.* **1999**, *19* (1−4), 659−672.
(27) Williams, E. R.; Henry, K. D.; McLafferty, F. W.; Shabanowitz, J.; Hunt, D. F., *J. Am. Soc. Mass Spectrom.* **1990**, *1* (5), 413−416.
(28) Spengler, B.; Kirsch, D.; Kaufmann, R.; Karas, M.; Hillenkamp, F.; Giessmann, U. *Rapid Commun. Mass Spectrom.* **1990**, *4* (9), 301−5.
(29) Wieghaus, A.; Schmidt, L.; Popova, A. M.; Komarov, V. V.; Jungclas, H. *Rapid Commun. Mass Spectrom.* **2000**, *14* (18), 1654−1661.

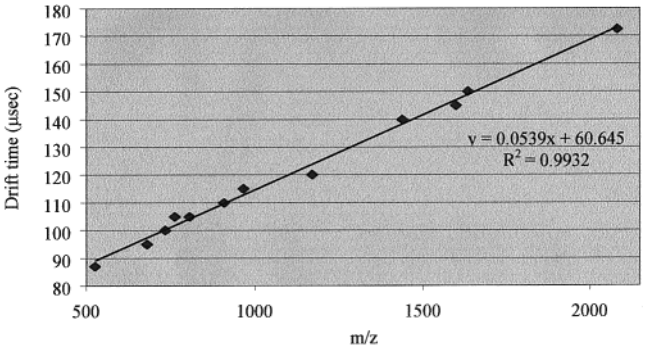


Figure 1. Drift time vs *m*/*z* value for selected peptide fragment ions formed by tryptic digestion of cytochrome *c*, taken from data shown in Figure 5. A linear relationship can be seen for the near-homologous series of peptides for the mass range typically observed for tryptic digest fragments.

WI) in 100% methanol (HPLC grade, Fisher). Without further cleanup, desalting, or separation, 2 $\mu$L of the digestion solution was added to 20 $\mu$L of the α-cyano/fructose matrix. Approximately 100 fmol of analyte was deposited on the sample probe using the dried droplet method at a 1000:1 matrix-to-analyte ratio. MALDI ions were formed at near-threshold levels using a 337-nm nitrogen laser operated at 20 Hz. Data were collected and signal averaged for 1−2 min. Data analysis was accomplished using Grams 3D and PROWL protein identification programs.

## RESULTS AND DISCUSSION

Before analyzing complex peptide mixtures, we analyzed a series of single-component samples to show that flight times through the drift cell increase near-linearly with increasing *m*/*z* of the peptide, i.e., to demonstrate that IM can be used as the primary mass analyzer. We also performed SID experiments on three model peptides to illustrate SID fragmentation efficiency and types of fragment ions produced from the digest fragment ions created by MALDI. Our SID results for peptides are very comparable to results reported previously by Wysocki.[30]

The mass-dependent mobilities for peptide ions are dominated by the hard-sphere collision cross-section term, i.e., volume-to-charge (*V*/*z*), and the ion−neutral interaction potential term can be neglected.[13] Figure 1 contains a plot of experimentally measured drift time versus *m*/*z* for 12 peptide fragment ions obtained by digestion of cytochrome *c* with trypsin (vide infra). The *y*-intercept corresponds to the flight time of an ion in the absence of a neutral bath gas. Clemmer and co-workers have shown similar data for singly charged peptide ions formed by electrospray ionization,[31] and the results shown in Figure 1 simply confirm their observations and the earlier work by Griffin[14] and Karpas.[15]

Figure 2 contains the SID spectrum of the hexapeptide HLGLAR (*m*/*z* 666.8). For simplicity we have only labeled the b- and y-fragment ions. Unassigned peaks are largely due to the loss of water or ammonia. The spectrum was acquired under conditions (20-eV collision energy) that are sufficient to obtain an almost complete SID fragmentation series for a low-mass parent. The

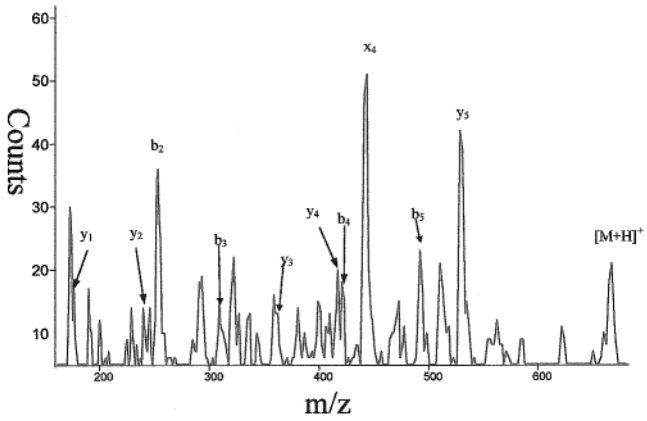


Figure 2. MALDI-IM-SID-o-TOF spectrum of HLGLAR. Mass accuracy for labeled SID fragments is ±1 amu. Collision energy is ~20 eV. A complete $y_j$ series and a near-complete $b_i$ series are shown. SID fragments resulting from small neutral losses ($H_2O$ and $NH_3$) are not labeled.

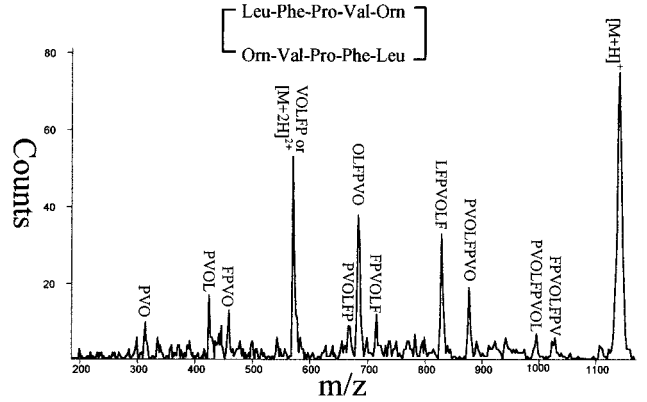


Figure 3. MALDI-IM-SID-o-TOF spectrum of gramicidin S. Mass accuracy for labeled SID fragments is ±1 amu. Collision energy is ~20 eV. Note the near-complete series of proline N-terminal fragments. The pentapeptide fragment VLOFP may be a combination of all five possible N-terminal fragments and the $[M + 2H]^{2+}$ parent ion, but is most likely PVOLF.

results are in excellent agreement with those of Kaiser et al.[32] The spectrum contains a complete series of y-type fragment ions ($y_1$−$y_5$) and most of the expected b-type ($b_2$−$b_4$) fragment ions. The $x_4$ fragment ion is the base peak in the spectrum, but it is not clear as to why this rather unusual cleavage is favored. The C-terminal arginine residue probably influences this. Although it is not unusual to see y-type fragment ions when arginine is on the C-terminus, it is rather unusual to see x-type ions in preference to y-type. We are currently exploring this issue further to determine whether this is due to the SID process (e.g., the internal energies of the ions following SID) or whether the secondary structure of this peptide ion is an important factor.[33]

Figure 3 contains the SID spectrum of the cyclic peptide gramicidin S (*m*/*z* 1142.5). This spectrum is very similar (in terms of fragment ion yields) to the SID spectrum of gramicidin S reported by McLafferty and co-workers.[34] Because gramicidin S

(30) Dongre, A. R.; Somogyi, A.; Wysocki, V. H. *J. Mass Spectrom.* **1996** *31*, 339−350.
(31) Hoaglund-Hyzer, C. S.; Li, J.; Clemmer, D. E. *Anal. Chem.* **2000**, *72* (13), 2737−2740.
(32) Kaiser, R. E., Jr.; Cooks, R. G.; Syka, J. E. P.; Stafford, G. C., Jr. *Rapid Commun. Mass Spectrom.* **1990**, *4* (1), 30−33.
(33) Gimon-Kinsel, M. E.; Barbacci, D. C.; Russell, D. H. *J. Mass Spectrom.* **1999**, *34*, 124−136.
(34) Chorush, R. A,; Little, D. P.; Beu, S. C.; Wood, T. D.; McLafferty, F. W. *Anal. Chem.* **1995**, *67* (6), 1042−1046.

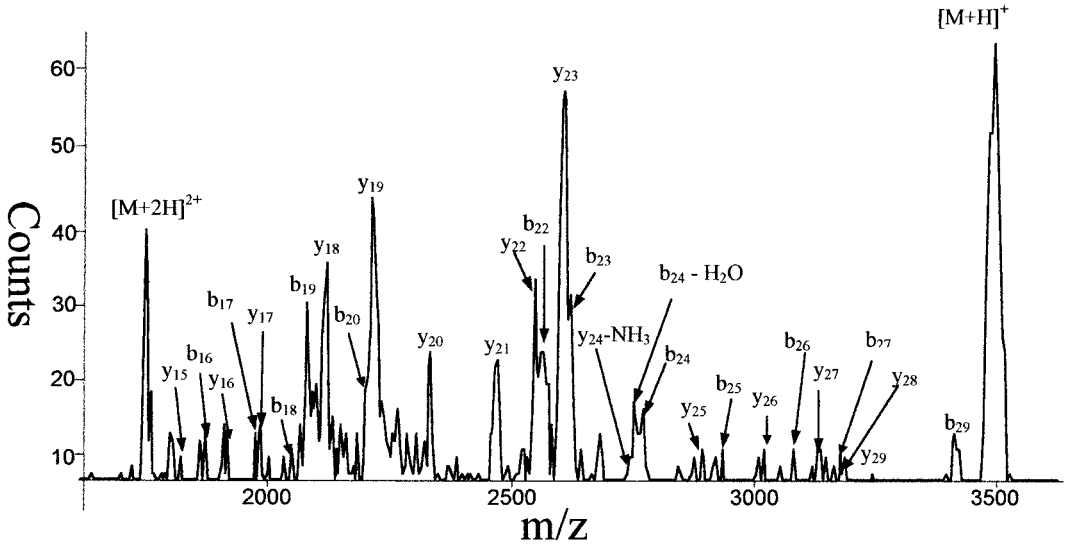


Figure 4. MALDI-IM-SID-o-TOF spectrum of bovine insulin b chain. The presence of the $[M + 2H]^{2+}$ ion is attributed to protonation of the $[M + H]^{+}$ during or immediately following the SID event. Mass accuracy for labeled SID fragments is ±1 amu. Collision energy is ~20 eV.

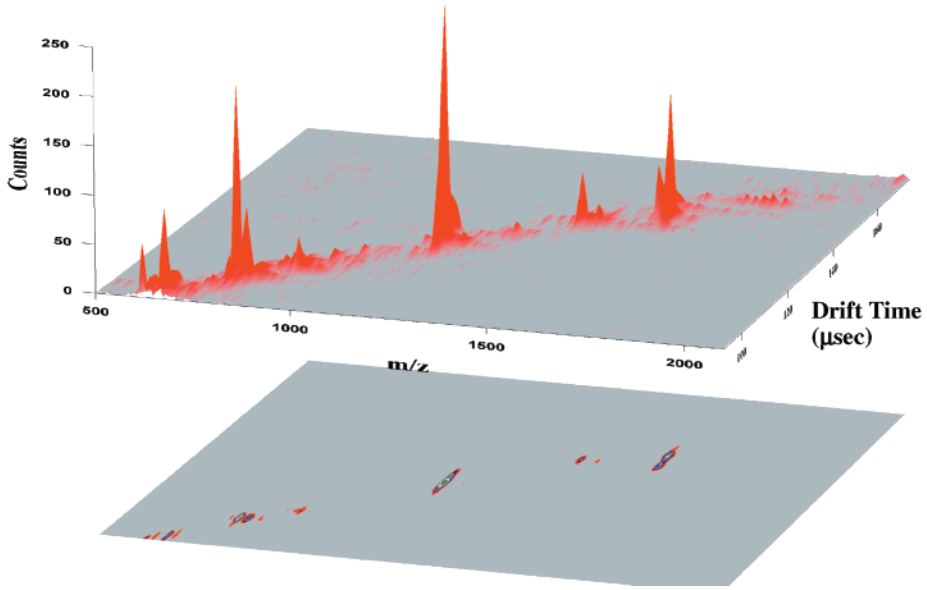


Figure 5. MALDI-IM-o-TOF of an "in-solution" digest of cytochrome *c* illustrating peptide mass mapping capability of the current instrument configuration. All ions entering the extraction region of the o-TOF are mass analyzed.

is a cyclic peptide, the SID fragment ions produced depend on the site of ring opening as opposed to the amino acid sequence; therefore, this spectrum is included to illustrate the efficiency of SID for producing fragment ions from a relatively stable peptide ion. Figure 4 contains the SID spectrum of protonated bovine insulin b chain ($m/z$ 3495.5). In addition to the single and doubly charged parent ions, the $y_{15}-y_{29}$ fragment series and the $b_{16}-b_{29}$ fragment ions are observed. These two ion series provide a complete sequence of the peptide. For example, the $y_{15}-y_{29}$ fragment ions can be used to determine the first 14 amino acids from the N-terminus, whereas the $b_{16}-b_{29}$ ions identify the remaining amino acids.

Figure 5 contains a plot of MALDI-IM-o-TOF-MS data for an "in-solution" digest of cytochrome *c*. $m/z$ data are represented on the *x*-axis, the *y*-axis is the total drift time for each digest fragment ion, and the *z*-axis is the total ion count. This data format is actually a 2-D (mobility and $m/z$) display of a peptide mass map. The data shown are typical for thermally denatured[35] tryptic protein digests. The digest and SID fragments listed in Table 1 were identified by searching the protein database (Swis-Prot) and using the Protein Prospector MSFit program. These peptide fragments account for 91 of the 104 (87.5% coverage) amino acids present in cytochrome *c*.

Four prominent digest fragments in the 2-D peptide mobility/mass map (Figure 6) were selected by ion mobility ($MS^1$), subjected to SID, and then analyzed by o-TOF-MS. The SID fragment ions have the same mobility as the parent ion, because the fragment ions are formed after the $[M + H]^{+}$ ions elute the drift cell. The time scale of an IM separation, 100 μs−20 ms, is 1−2 orders of magnitude longer than the flight times in the mass spectrometer (10−100 μs). Consequently, it is possible to acquire SID fragment ion spectra for all ions eluting the drift cell from a single ionization event. The SID was performed using the same method as was used for the single-component peptide samples.

(35) Park, Z. Y.; Russell, D. H. *Anal. Chem.* **2000**, *72* (11), 2667−2670.

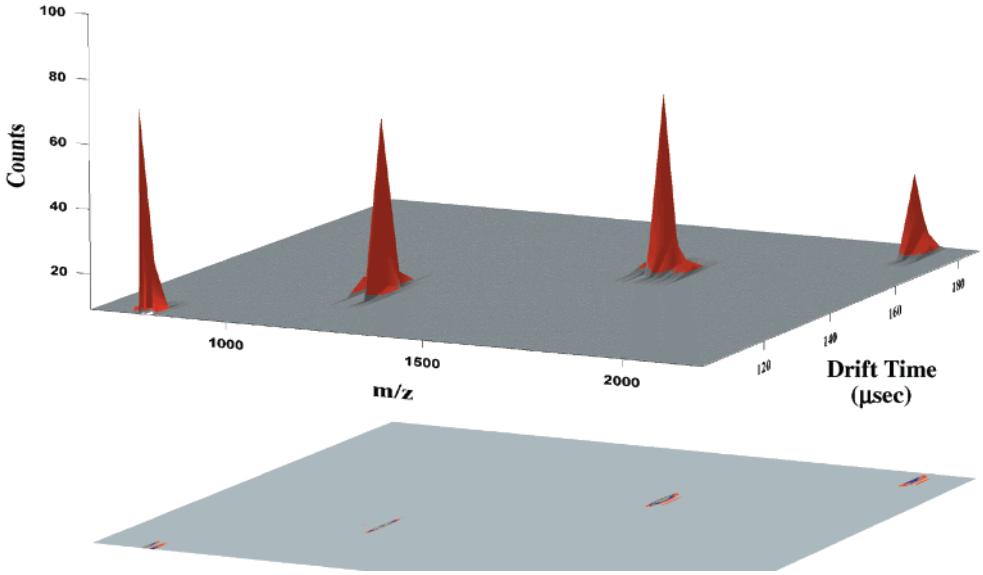


Figure 6. MALDI-IM-o-TOF of four mobility-selected tryptic fragments from an "in-solution" digest of cytochrome *c*. Mobility selection of ions eluting from the drift cell for subsequent mass analysis is accomplished using the arrival times predicted by the trend observed in Figure 1 to operate the extraction plates of the o-TOF mass spectrometer.

Table 1. A List of Assigned Fragment Ions, *m*/*z* Values, and Amino Acid Sequences of Peptide Fragments from the Tryptic Digestion of Cytochrome *c*

| digest/ SID fragment | *m*/*z* [M + H]$^+$ calc | exp | amino acid sequence |
|---|---|---|---|
| peak A | 780.0 | 778.9 | MIFAGIK |
| $y_6$ | 648.8 | 648.0 | IFAGIK |
| $b_6$ | 633.8 | 633.7 | MIFAGI |
| $y_5$ | 535.7 | 534.4 | FAGIK |
| peak B | 1169.3 | 1168.6 | TGPNLHGLFGR |
| $y_{10}$ | 1068.2 | 1068.4 | GPNLHGLFGR |
| $y_9$ | 1011.2 | 1010.6 | PNLHGLFGR |
| $b_{10}$ | 995.1 | 994.2 | TGPNLHGLFG |
| $b_9$ | 938.1 | 937.5 | TGPNLHGLF |
| $y_8$ | 914.1 | 913.5 | NLHGLFGR |
| $y_7$ | 799.9 | 799.6 | LHGLFGR |
| $b_8$ | 790.9 | 789.8 | TGPNLHGL |
| $y_6$ | 686.6 | 685.9 | HGLFGR |
| $b_7$ | 677.4 | 678.7 | TGPNLHG |
| $b_6$ | 620.7 | 619.9 | TGPNLH |
| peak C | 1634.9 | 1635.2 | CAQCHTVEK + heme |
| $y_8$ + heme | 1531.8 | 1530.9 | AQCHTVEK + heme |
| $b_8$ + heme | 1488.7 | 1487.8 | CAQCHTVE + heme |
| $y_7$ + heme | 1460.7 | 1461.1 | QCHTVEK + heme |
| $b_7$ + heme | 1359.6 | 1360.1 | CAQCHTV + heme |
| $y_6$ + heme | 1332.5 | 1311.6 | CHTVEK + heme |
| $b_6$ + heme | 1260.5 | 1259.8 | CAQCHT + heme |
| peak D | 2082.4 | 2083.2 | GITWKEETLMEYLENPK |
| $y_{16}$ | 2025.3 | 2026.0 | ITWKEETLMEYLENPK |
| $b_{16}$ | 1936.2 | 1936.8 | GITWKEETLMEYLENP |
| $y_{15}$ | 1912.2 | 1913.1 | TWKEETLMEYLENPK |
| $b_{15}$ | 1839.1 | 1840.2 | GITWKEETLMEYLENPK |
| $b_{14}$ | 1725.0 | 1725.7 | GITWKEETLMEYLE |

The SID collision energy was held constant (20 eV); however, since the fragmentation efficiency is a function of velocity, it would be useful to program a voltage ramp (e.g., increasing SID energy with increasing *m*/*z* for more fragmentation coverage) into this experiment. Figure 7 contains a 2-D plot of the IM-SID-o-TOF spectra, and Table 1 contains a list of the *m*/*z* values and assignments for the fragment ions. Note that the range of ions observed for digest peaks A and B in Figure 7 covers the mass range from *m*/*z* 500 up to the parent and that this is not the case for peaks C and D. We attribute the lack of low-mass ions in C and D to insufficient energy deposited in the parent ion due to the orientation of the SID surface. The grazing incidence angle does not permit energy conversion similar to that for FSAM-coated surfaces positioned at an angle to the incident ion beam. It is also high likely that MALDI-formed ions are formed with excess internal energy and that this affects the SID fragment ion yields. We see similar results for the photodissociation of MALDI-formed ions.[36] It should be noted that we do observe that low-*m*/*z* fragment ions increase in abundance at higher translational energies. For SID energies above 500 eV, Reiderer did not observe the large y- or b-type fragment ions seen in Figure 7, but rather significant single amino acid residue and immonium ion production.[37] Also notice the similarity between the fragmentation patterns and parent peak intensity observed for peak A (*m*/*z* 780) and that for HLGLAR (666.8) in Figure 2, peak B (*m*/*z* 1169) and gramicidin S (*m*/*z* 1142.5) in Figure 3, and peak D and bovine insulin b chain in Figure 4.

We have not listed all the fragment ions detected in the SID spectrum in Table 1. In particular, we omitted fragment ions that involved loss of $H_2O$ and $NH_3$ for $b_i$ and $y_j$ sequence fragment ions. Those listed are sufficient to identify the peptides and the protein from which the peptides are generated. For the database searches, TOF mass accuracy was set to ±1 Da for both [M + H]$^+$ ions and the *m*/*z* values of the SID fragment ions, and ion types were limited to b and y fragments. SID fragments were manually identified by matching experimentally measured fragment ion *m*/*z* values with predicted *m*/*z* values. We are currently developing a computer algorithm to perform this task.

The *m*/*z* 649 SID fragment from digest fragment A (Figure 7; *m*/*z* 780) corresponds to loss of a methionine residue ($y_6$). If we

(36) Hettick, J. M.; Russell, D. H. submitted for publication in *Anal. Chem.*
(37) Reiderer, D. E, Haney, L. L.; Hilgenbrink, A. R.; Beck, J. R. *The 48th ASMS Conf. Mass Spectrom. Allied Top.*, Long Beach, CA, 2000.

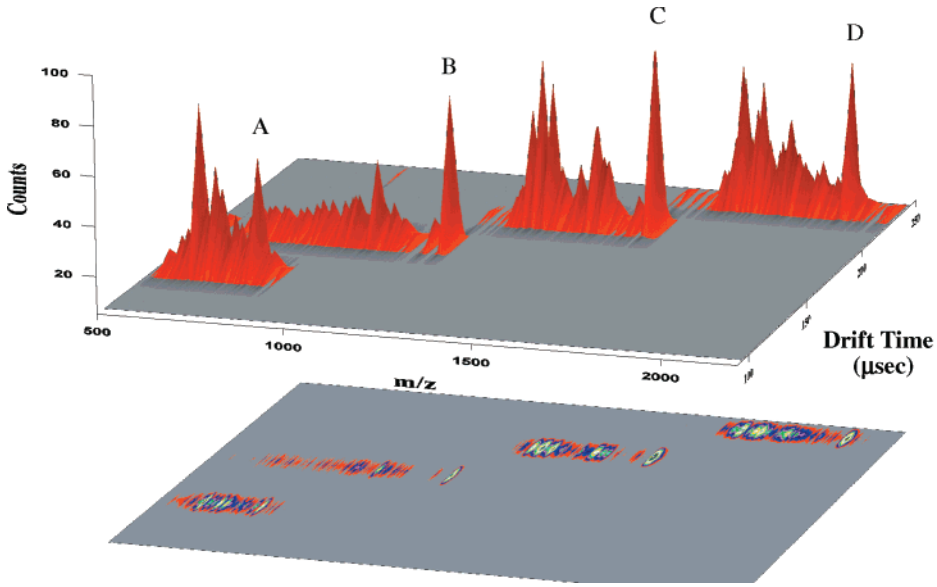


Figure 7. MALDI-IM-SID-o-TOF spectra of four mobility-selected peaks from an "in-solution" digest of cytochrome *c*. Mass accuracy for labeled SID fragments is ±1 amu. Collision energy is ~20 eV. SID fragments are associated by total mobility drift time with the parent digest fragment. The data handling package allows for any of the four spectra to be observed in a format similar to the other figures for ease of peak assignment.

search the database using the $m/z$ of the $[M + H]^+$ ion and the $y_6$ fragment using PROWL's PepFrag routine, we obtain a match against 17 proteins, where 10 of the matches are cytochrome *c*. If we add two additional SID fragments, e.g., $m/z$ 634 ($y_5$) and 536 ($b_6$), the number of protein matches is reduced to 11, where 10 are species-nonspecific cytochrome *c*. The sequences returned were MIFAGIK for cytochrome *c* and MIMKEK for IL4_TURTR interleukin-4 precursor. Because the MIFAGIK digest fragment is conserved from species to species, the database-identified proteins would not be species specific.

The same procedures were used to identify the remaining three peaks in the 2-D peptide mass map. Digest fragment labeled B ($m/z$ 1169) was identified using $m/z$ 1068 and 1011 SID fragment ions, and we obtained 10 matches, where 9 of the matches were conserved sequences for cytochrome *c*. If we added the $m/z$ 995 SID fragment to the search, 10 species-nonspecific matches for cytochrome *c* were obtained. The complete sequence for peak B can be determined from the fragment ion spectrum (Table 1); e.g., the fragment ion series $b_6-b_{10}$ and $y_6-y_{10}$ can be used to identify the complete sequence.

The database search to identify peak C ($m/z$ 1634) resulted in zero matches for $m/z$ 1532, 1489, 1461, and 1359; however, we previously reported that the $m/z$ 1634 ion was most probably a heme-containing fragment ion.[38] Subtracting the isotope-averaged mass of heme (615.7) from the measured $m/z$ values, including the $[M + H]^+$ ion, yields $m/z$ 915.2 (1530.9−615.7), 872.1 (1487.8−615.7), 845.4 (1461.1−615.7), and 744.4 (1360.1−615.7), and the database search produces 10 matches all of which are cytochrome *c*. Thus, the peptide sequence for peak C is CAQCHTVEK + heme, which corresponds to amino acid residues 14−22. Peak D was identified as equine cytochrome *c* on the basis of the $[M + H]^+$ ion, $m/z$ 2082, and three SID fragments, $m/z$ 2025, 1935, and 1912. The use of fewer numbers of SID fragment ion $m/z$ values for peak D resulted in identification as nonspecies-specific cytochrome *c*.

(38) Russell, D. H.; Edmondson, R. D. *J. Mass Spectrom.* **1997**, *32* (3), 263−276.

## CONCLUSIONS

In this paper, we demonstrate that peptide mass mapping and sequencing can be accomplished with MALDI-IM-SID-o-TOF-MS. The peptide mass mapping and SID peptide data are comparable to that obtained using more conventional mass spectrometry techniques. The advantages of MALDI-IM-SID-o-TOF-MS are sample throughput and simultaneous acquisition of the peptide mass map and sequence analysis. Future work will be directed toward improving both mobility and mass resolution of the prototype instrument, automation of sample handling,, and comparison of collision-induced dissociation, photodissociation, and SID for peptide sequencing.

## ACKNOWLEDGMENT

The TOF development research (TAMU) is supported by a grant from the U.S. Department of Energy, Division of Chemical Sciences, Basic Energy Science, and the ion mobility research (TAMU) is supported by a grant from the National Science Foundation. The Ion Mobility/TOF developmental research is supported by a NIH-SBIR grant (Ionwerks). The authors acknowledge Zee-Yong Park's assistance in the protein digestion and peptide mass mapping studies and Kenneth Greer for technical assistance with instrument development and construction.

Received for review December 5, 2000. Accepted March 7, 2001.

AC001430A